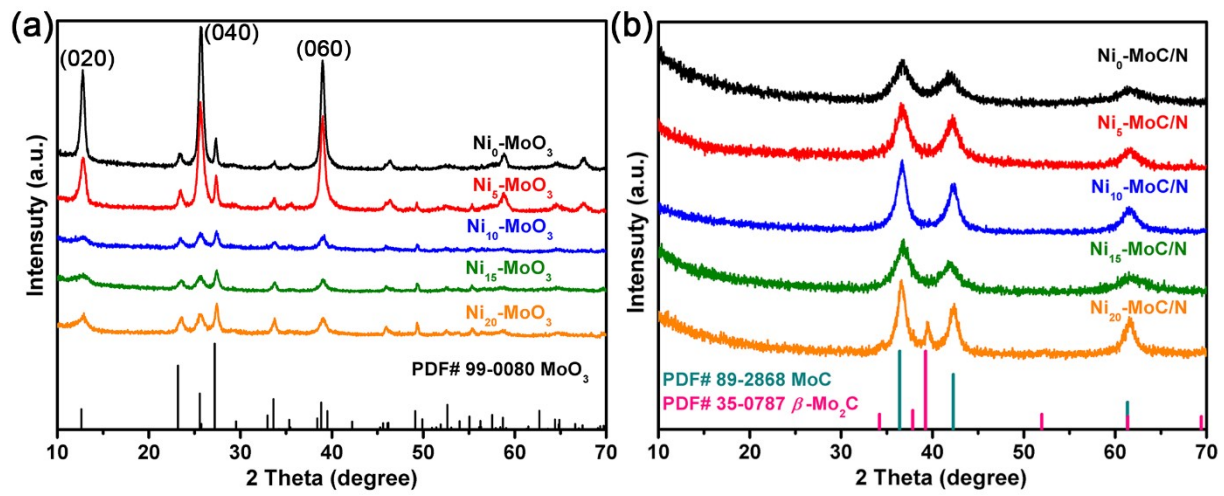


## Supporting Information

### **Ni-directed biphasic N-doped Mo<sub>2</sub>C as efficient hydrogen evolution catalysts in both acidic and alkaline conditions**

*Cheng-Feng Du, Yaxin Wang, Xiangyuan Zhao, Jinjin Wang, Xiaomei Wang, Weigang Wang, and Hong Yu\**



**Figure S1.** XRD patterns of (a)  $\text{Ni}_x\text{-MoO}_3$  nanobelts, and (b)  $\text{Ni}_x\text{-MoC/N}$  intermedia.

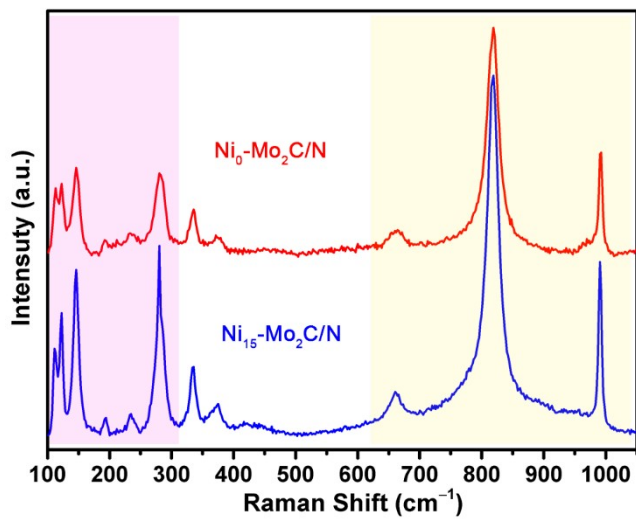


**Figure S2.** Raman spectrum of  $\text{Ni}_0\text{-Mo}_2\text{C/N}$  and  $\text{Ni}_{15}\text{-Mo}_2\text{C/N}$ .

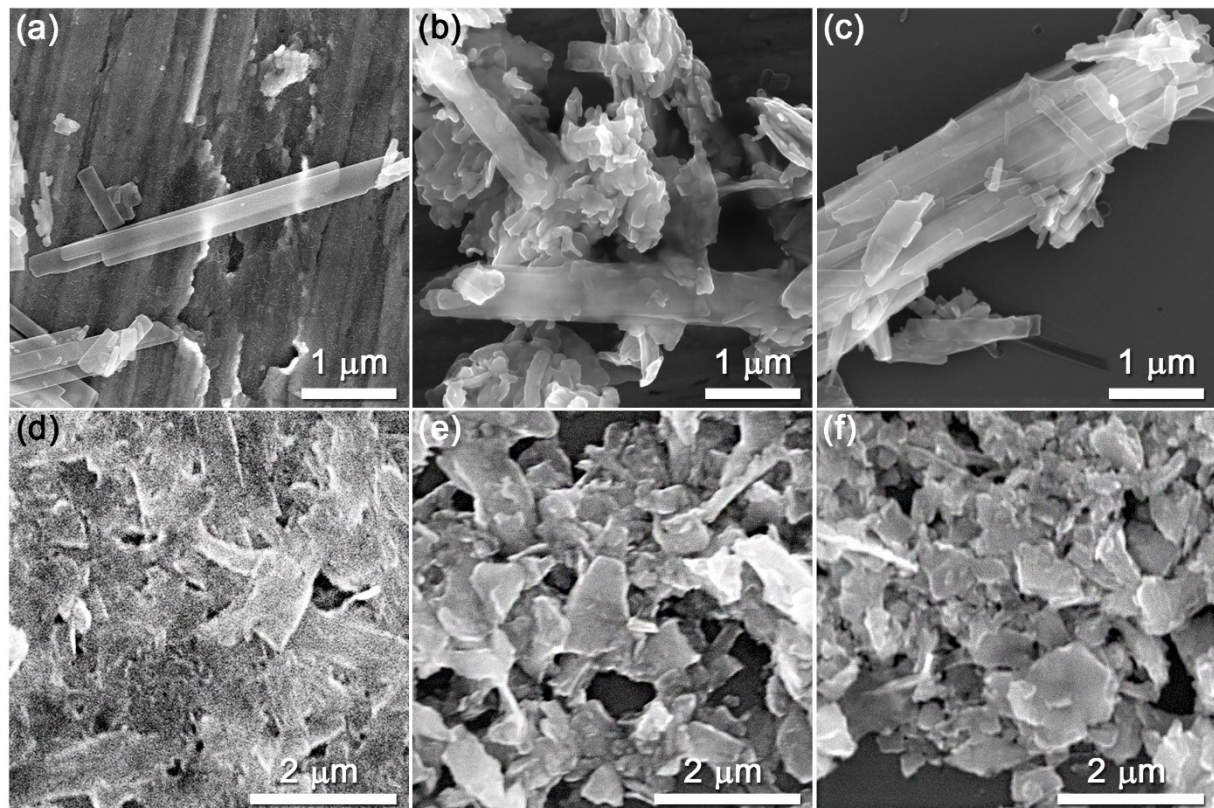


**Figure S3.** SEM imagines of (a) Ni<sub>0</sub>-MoO<sub>3</sub>, (b) Ni<sub>0</sub>-MoC/N, (c) Ni<sub>0</sub>-Mo<sub>2</sub>C/N, (d) Ni<sub>15</sub>-MoO<sub>3</sub>; (e) Ni<sub>15</sub>-MoC/N, and (f) Ni<sub>15</sub>-Mo<sub>2</sub>C/N.

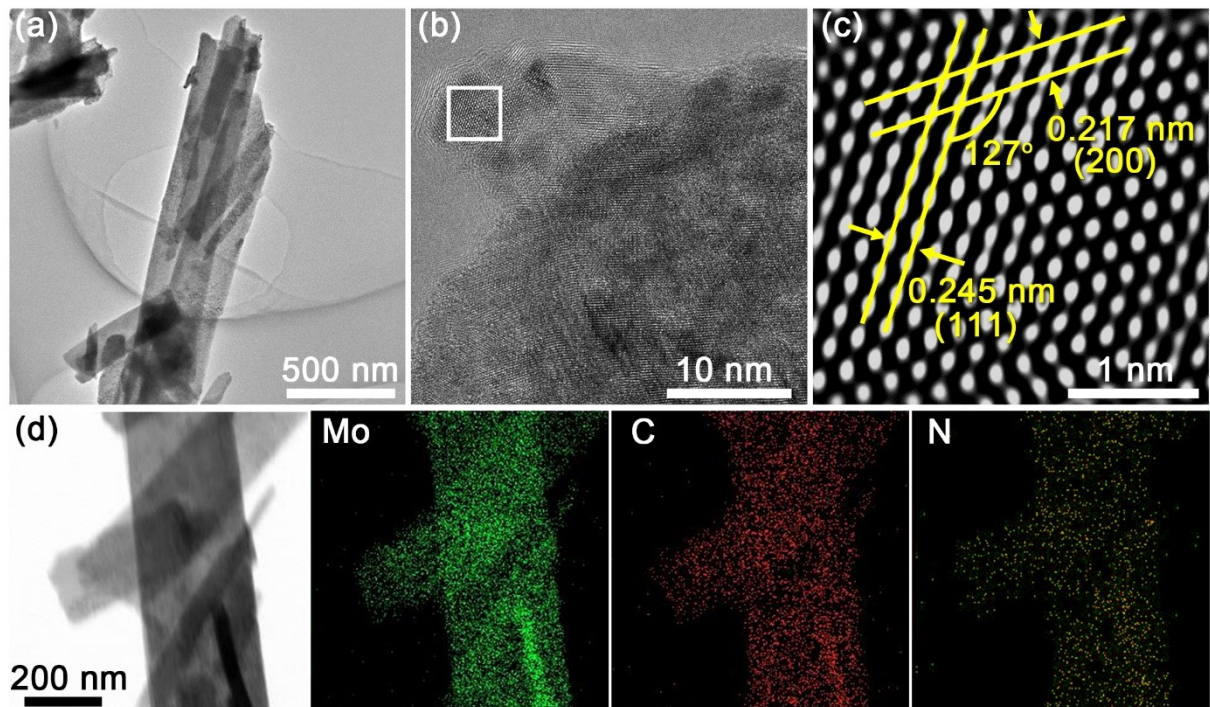


**Figure S4.** (a) TEM and (b) HRTEM image of  $\text{Ni}_0\text{-Mo}_2\text{C}/\text{N}$ . (c) The inverse FFT image of the region which labeled in (b). (d) Elemental mappings (Mo, C and N elements) of the  $\text{Ni}_0\text{-Mo}_2\text{C}/\text{N}$ .

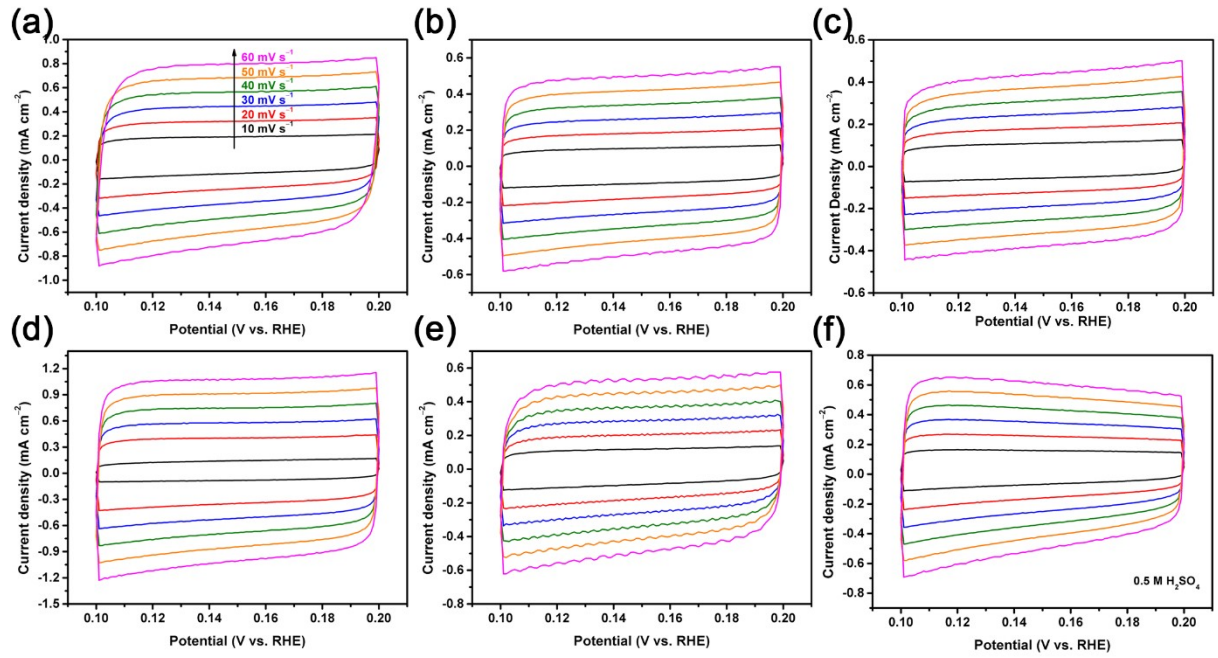


**Figure S5.** CV curves of the electrocatalysts: (a) Ni<sub>0</sub>-Mo<sub>2</sub>C/N; (b) Ni<sub>5</sub>-Mo<sub>2</sub>C/N; (c) Ni<sub>10</sub>-Mo<sub>2</sub>C/N; (d) Ni<sub>15</sub>-Mo<sub>2</sub>C/N; (e) Ni<sub>20</sub>-Mo<sub>2</sub>C/N, and (f) 20% Pt/C, which were measured at various scan rates of 10, 20, 30, 40, 50, and 60 mV s<sup>-1</sup> in 0.5 M H<sub>2</sub>SO<sub>4</sub>.

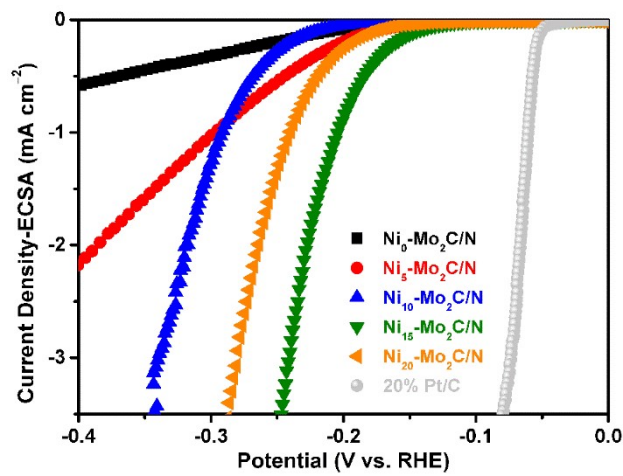


**Figure S6.** Normalized LSV curves by ECSA of the electrocatalysts in 0.5 M H<sub>2</sub>SO<sub>4</sub>.

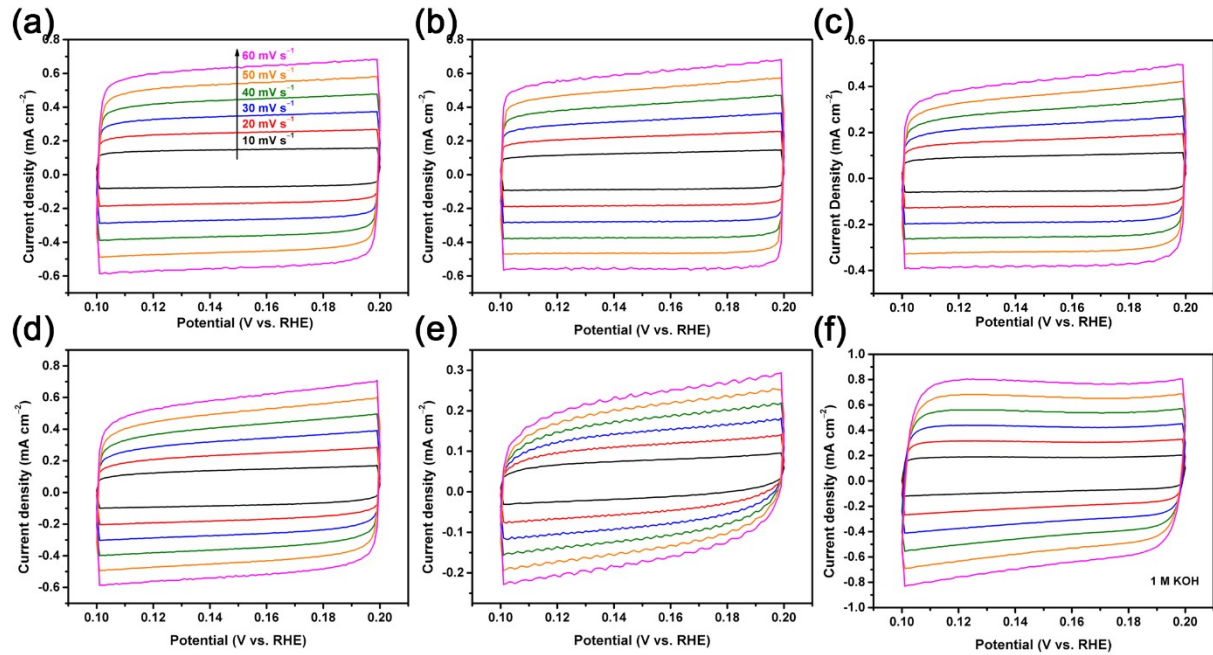


**Figure S7.** CV curves of the electrocatalysts: (a) Ni<sub>0</sub>-Mo<sub>2</sub>C/N; (b) Ni<sub>5</sub>-Mo<sub>2</sub>C/N; (c) Ni<sub>10</sub>-Mo<sub>2</sub>C/N; (d) Ni<sub>15</sub>-Mo<sub>2</sub>C/N; (e) Ni<sub>20</sub>-Mo<sub>2</sub>C/N, and (f) 20% Pt/C, which were measured at various scan rates of 10, 20, 30, 40, 50, and 60 mV s<sup>-1</sup> in 1 M KOH.

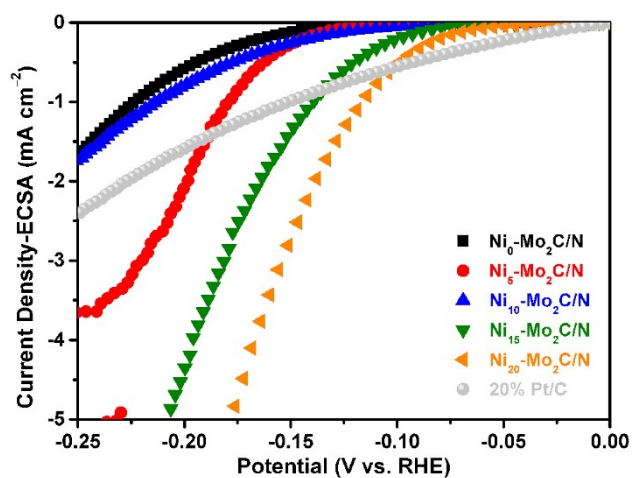


**Figure S8.** Normalized LSV curves by ECSA of the electrocatalysts in 1 M KOH.

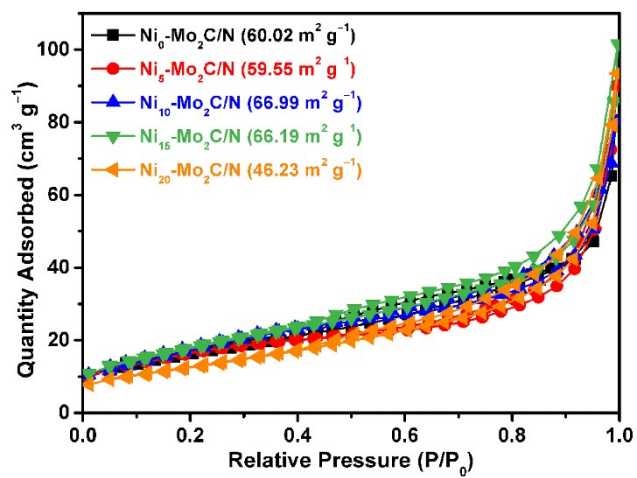


**Figure S9.** N<sub>2</sub> adsorption-desorption isotherms of the series Ni<sub>x</sub>-Mo<sub>2</sub>C/N electrocatalysts.

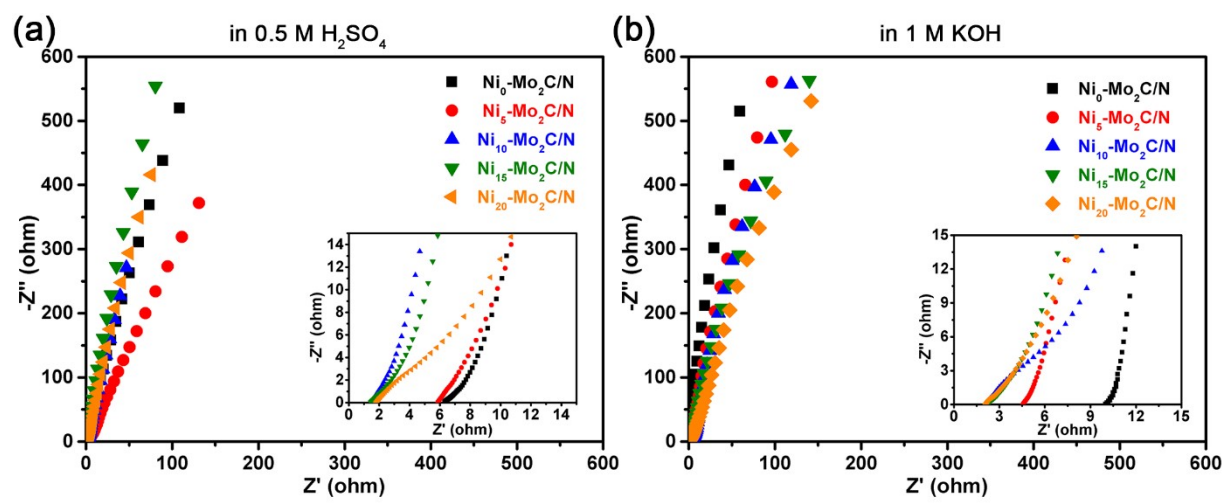


**Figure S10.** Nyquist plots of  $\text{Ni}_x\text{-Mo}_2\text{C/N}$  in (a) 0.5 M  $\text{H}_2\text{SO}_4$ ; (b) 1 M KOH.

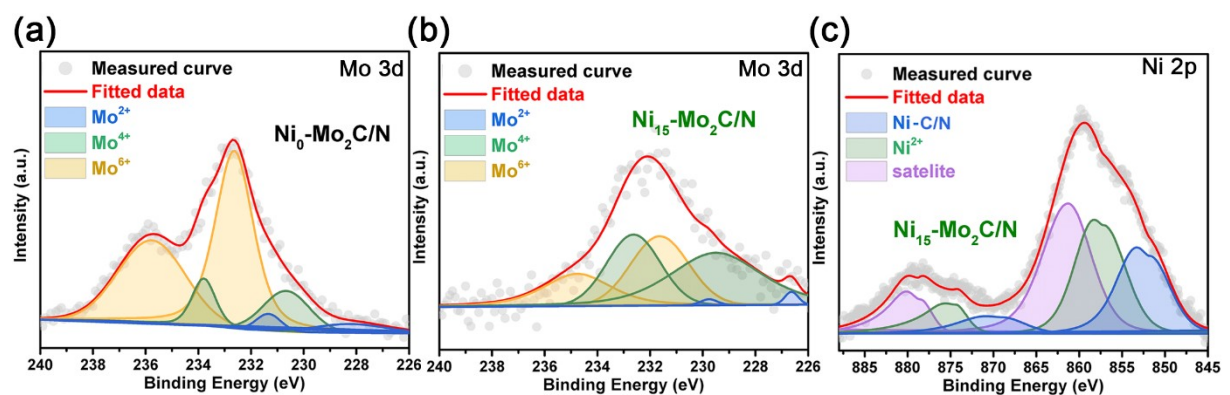


**Figure S11.** The high-resolution XPS spectra after stability test in 1M KOH: (a) Mo 3d spectrum of Ni<sub>0</sub>-Mo<sub>2</sub>C/N, (b) Mo 3d and (c) Ni 2p spectra of Ni<sub>15</sub>-Mo<sub>2</sub>C/N.

**Table S1** Comparison of element contents in Mo<sub>2</sub>C/N, 15% Ni-Mo<sub>2</sub>C/N from EDS results.

Samples	Atomic Fraction (%)			
	C	N	Mo	Ni
Mo <sub>2</sub> C/N	56.89	6.67	36.44	-
15% Ni-Mo <sub>2</sub> C/N	60.53	2.90	35.86	0.71

**Table S2** The comparison of HER performance for different catalysts in literatures.

Samples	Overpotential (mV)		Tafel Slopes (mV/dec)		References
	0.5M H <sub>2</sub> SO <sub>4</sub>	1M KOH	0.5M H <sub>2</sub> SO <sub>4</sub>	1M KOH	
Ni <sub>15</sub> -Mo <sub>2</sub> C/N	155	110	56.9	46.5	This work
Mo <sub>2</sub> C,Mo <sub>2</sub> N/N,P-rGO	195	115	60	57	[2]
Mo <sub>2</sub> C@C	170	119	58	51	[3]
Mo <sub>0.84</sub> Ni <sub>0.16</sub> -Mo <sub>2</sub> C/NCNFs	229	183	76	71	[4]
Mo <sub>2</sub> C@BNC	184	145	68.3	57.4	[5]
Mo <sub>2</sub> C	235	152	70.5	40.2	[6]
Mo <sub>2</sub> C/NCF	144	100	55	65	[7]
Mo/Mo <sub>2</sub> C/N-CNFs	175	162	64.6	47.9	[8]
Fe-Mo <sub>2</sub> C@NCF	65	129	110	76	[9]
Ni <sub>0.5</sub> @MoC <sub>x</sub> /NC	100	150	53.2	76.1	[10]
PMTC-7HA	172	219	56.2	63.3	[11]
Ni-N-MoC <sub>x</sub>	163	124	69.32	106.74	[12]
m-Mo <sub>2</sub> C/G	135	128	58	56	[13]
Ni <sub>0.5</sub> @MoC <sub>x</sub> /NC	100	150	53.2	74.6	[14]
Ni@Mo <sub>2</sub> C-HC800	192	123	98	83	[15]
Mo <sub>0.84</sub> Ni <sub>0.16</sub> -Mo <sub>2</sub> C/NCNFs	-	183	-	71	[16]
Ni-GF/Mo <sub>2</sub> C	158	189	159	64	[17]
30 wt.% Ni-MO <sub>2</sub> C-R,	-	120	-	49	[18]

**Table S3** The internal resistance tested before and after CV in acidic and alkaline conditions.

Samples	0.5 M H <sub>2</sub> SO <sub>4</sub> (Ω)		1 M KOH (Ω)	
	Before	After	Before	After
Ni <sub>0</sub> -Mo <sub>2</sub> C/N	6.31	12.60	10.00	6.42
Ni <sub>5</sub> -Mo <sub>2</sub> C/N	5.87	5.88	4.56	3.71
Ni <sub>10</sub> -Mo <sub>2</sub> C/N	1.49	1.52	2.14	2.11
Ni <sub>15</sub> -Mo <sub>2</sub> C/N	1.45	1.46	2.19	2.19
Ni <sub>20</sub> -Mo <sub>2</sub> C/N	1.81	1.79	2.09	2.03

## Reference

- [1]. C.-F. Du, X. Sun, H. Yu, Q. Liang, K. N. Dinh, Y. Zheng, Y. Luo, Z. Wang, Q. Yan, Synergy of Nb Doping and Surface Alloy Enhanced on Water–Alkali Electrocatalytic Hydrogen Generation Performance in Ti-Based MXene. *Adv. Sci.*, 2019. 6(11), 1900116.
- [2]. Y. I. Kurys, D. O. Mazur, V. G. Koshechko, V. D. Pokhodenko, Nanocomposite Based on N,P-Doped Reduced Graphene Oxide, Mo<sub>2</sub>C, and Mo<sub>2</sub>N as Efficient Electrocatalyst for Hydrogen Evolution in a Wide pH Range. *Electrocatalysis*, 2021. 12(5), 469-477.
- [3]. Y. Zhao, S. Wang, H. Liu, X. Guo, X. Zeng, W. Wu, J. Zhang, G. Wang, Porous Mo<sub>2</sub>C nanorods as an efficient catalyst for the hydrogen evolution reaction. *Journal of Physics and Chemistry of Solids*, 2019. 132, 230-235.
- [4]. L. Ying, S. Sun, W. Liu, H. Zhu, Z. Zhu, A. Liu, L. Yang, S. Lu, F. Duan, C. Yang, M. Du, Heterointerface engineering in bimetal alloy/metal carbide for superior hydrogen evolution reaction. *Renewable Energy*, 2020. 161, 1036-1045.
- [5]. S. Wu, M. Chen, W. Wang, J. Zhou, X. Tang, D. Zhou, C. Liu, Molybdenum carbide nanoparticles assembling in diverse heteroatoms doped carbon matrix as efficient hydrogen evolution electrocatalysts in acidic and alkaline medium. *Carbon*, 2021. 171, 385-394.
- [6]. Y. Wang, W. Hong, C. Jian, X. He, Q. Cai, W. Liu, The intrinsic hydrogen evolution performance of 2D molybdenum carbide. *Journal of Materials Chemistry A*, 2020. 8(45), 24204-24211.
- [7]. Y. Huang, Q. Gong, X. Song, K. Feng, K. Nie, F. Zhao, Y. Wang, M. Zeng, J. Zhong, Y. Li, Mo<sub>2</sub>C nanoparticles dispersed on hierarchical carbon microflowers for efficient electrocatalytic hydrogen evolution. *ACS Nano*, 2016. 10(12), 11337-11343.
- [8]. M. Li, H. Wang, Y. Zhu, D. Tian, C. Wang, X. Lu, Mo/Mo<sub>2</sub>C encapsulated in nitrogen-doped carbon nanofibers as efficiently integrated heterojunction electrocatalysts for hydrogen evolution reaction in wide pH range. *Applied Surface Science*, 2019. 496.
- [9]. J. Huang, J. Wang, R. Xie, Z. Tian, G. Chai, Y. Zhang, F. Lai, G. He, C. Liu, T. Liu, P. R. Shearing, D. J. L. Brett, A universal pH range and a highly efficient Mo<sub>2</sub>C-based electrocatalyst for the hydrogen evolution reaction. *Journal of Materials Chemistry A*, 2020. 8(38), 19879-19886.
- [10]. C. Liu, L. Sun, L. Luo, W. Wang, H. Dong, Z. Chen, Integration of Ni doping and a Mo<sub>2</sub>C/MoC heterojunction for hydrogen evolution in acidic and alkaline conditions. *ACS Applied Materials & Interfaces*, 2021. 13(19), 22646-22654.
- [11]. Y. Tang, C. Yang, M. Sheng, X. Yin, W. Que, J. Henzie, Y. Yamauchi, Phosphorus-doped molybdenum carbide/MXene hybrid architectures for upgraded hydrogen evolution reaction performance over a wide pH range. *Chemical Engineering Journal*, 2021. 423, 130183.
- [12]. J. Chen, J. Jia, Z. Wei, G. Li, J. Yu, L. Yang, T. Xiong, W. Zhou, Q. Tong, Ni and N co-doped MoC<sub>x</sub> as efficient electrocatalysts for hydrogen evolution reaction at all-pH values. *International Journal of Hydrogen Energy*, 2018. 43(31), 14301-14309.
- [13]. L. Huo, B. Liu, G. Zhang, J. Zhang, Universal strategy to fabricate a two-dimensional layered mesoporous Mo<sub>2</sub>C electrocatalyst hybridized on graphene sheets with high activity and durability for hydrogen generation. *ACS Applied Materials & Interfaces*, 2016. 8(28), 18107-18118.

- [14]. C. Liu, L. Sun, L. Luo, et al. Integration of Ni doping and a Mo<sub>2</sub>C/MoC heterojunction for hydrogen evolution in acidic and alkaline conditions[J]. ACS Appl Mater Interfaces, 2021, 13(19), 22646-22654.
- [15]. X. Xu, F. Nosheen, X. Wang. Ni-decorated molybdenum carbide hollow structure derived from carbon-coated metal–organic framework for electrocatalytic hydrogen evolution reaction. Chemistry of Materials, 2016, 28(17), 6313-6320.
- [16]. L. Ying, S. Sun, W. Liu, et al. Heterointerface engineering in bimetal alloy/metal carbide for superior hydrogen evolution reaction, Renewable Energy, 2020, 161, 1036-1045.
- [17]. C. Yang, R. Zhao, H. Xiang, et al. Ni-activated transition metal carbides for efficient hydrogen evolution in acidic and alkaline solutions, Advanced Energy Materials, 2020, 10(37), 2002260-2002270.
- [18]. P. Xiao, Y. Yan, X. Ge, et al. Investigation of molybdenum carbide nano-rod as an efficient and durable electrocatalyst for hydrogen evolution in acidic and alkaline media[J]. Applied Catalysis B: Environmental, 2014, 154-155, 232-237.